Reliability in Post-Disaster Networks: A Novel Interference-Mitigation Strategy

Reliability in Post-Disaster Networks: A Novel Interference-Mitigation Strategy

Maurilio Matracia (Student Member, IEEE), Mustafa A. Kishk (Member, IEEE), and Mohamed-Slim Alouini (Fellow, IEEE)

Abstract

We hereby present a novel interference mitigation strategy specifically designed to enhance the quality of service that a typical terrestrial user equipment (UE) would experience after the occurrence of a calamity. In particular, we devise a novel stochastic geometry framework where the functioning ground base stations are modeled as an inhomogeneous Poisson point process, and promote proper silencing as an effective solution to improve both coverage and reliability (which is usually overlooked in emergency scenarios); in particular, the latter is evaluated by means of the signal-to-interference-plus-noise ratio (SINR) meta distribution performance metric. The derived downlink performances assume Rayleigh fading conditions for all wireless links. The numerical results show insightful trends in terms of both average coverage probability (which is optimized by choosing the best area for applying the silencing strategy) and SINR meta distribution, depending on: distance of the UE from the disaster epicenter (henceforth intended as the center of the area where the BS can be damaged), disaster radius (also referring to the latter area), and quality of resilience of the terrestrial network. The aim of this paper is therefore to prove the effectiveness of proper silencing in emergency scenarios, at least from the coverage and reliability perspectives.

Index Terms

Silencing, SINR meta distribution, coverage probability, stochastic geometry, post-disaster communications.

Maurilio Matracia and Mohamed-Slim Alouini are with the Computer, Electrical, and Mathematical Sciences and Engineering (CEMSE) Division at King Abdullah University of Science and Technology (KAUST), Thuwal, Kingdom of Saudi Arabia (KSA) (email: {maurilio.matracia; slim.alouini}@kaust.edu.sa).

Mustafa Kishk is with the Department of Electronic Engineering, Maynooth University, Maynooth, W23 F2H6, Ireland (email: mustafa.kishk@mu.ie).

I. Introduction

Despite the authorities' efforts, the number of natural and human-made calamities per year still remains high mostly because of the rapid climate change and frequent political instabilities, respectively. Generally speaking, disasters have the potential to affect any form of life within the affected zone. Moreover, the occurrence of a calamity usually causes considerable damages to the cultural heritage and the economy of a community.

Based on similar considerations, more than thirty years ago, the United Nations (UN) established the *International Search and Rescue Advisory Group* (INSARAG) to pursue multiple goals, consisting in [1]:

- An improvement in the effectiveness of both emergency preparedness and response operations;
- Enhancing the search-and-rescue (SAR) activities in disaster-prone countries, as well as cooperation among international teams working on urban-SAR (USAR) missions;
- Developing USAR procedures, guidelines and best practices for post-disaster scenarios.

In emergency situations, both victims and first responders (FRs) usually need wireless connectivity to save their lives. However, terrestrial telecommunications infrastructures are quite susceptible to strong perturbations such as the ones usually originating from calamities. This means that connectivity easily becomes unavailable or insufficient over the disaster-struck area, because of the damages suffered by either cell towers or power grids feeding them. In particular, the main problems deriving from the dysfunction of the networking equipment include: larger ratio of packet losses, continuous routing tables' reconfiguration, and radio frequency (RF) signals' distortion [2], [3].

One interesting solution to restore the connectivity in such scenarios is to deploy ad hoc networks consisting of either terrestrial [4] or aerial [5] platforms. However, it is evident that this solution inherently brings some issues, such as the cost of the platforms (often accompanied by their technological limitations), the foresight of buying the platforms and devising a deployment strategy, and the time needed to deploy them.

Another important aspect that needs to be taken into account when talking about coverage in cellular networks regards the aggregate interference deriving from the densification of the network: this, in turn, represents a critical issue and implies a well known trade-off between the quality of the desired signal (which increases when reducing the minimum distance to the

tagged base station (BS)) and the strength of the aggregate interference (which increases with the number of surrounding interferers). Therefore, in this paper, we propose an interference mitigation strategy based on BS silencing, which can be applied at zero cost and in a timely manner.

A. Related Works

We categorize the works related to this paper into two categories: stochastic geometry (SG) for post-disaster communications (PDCs) and BS silencing.

1) SG for PDCs: SG is a powerful mathematical tool that allows to derive tractable models, which in turn can be implemented to study random phenomena on two or more dimensions. In the context of wireless networks, SG can be used to statistically assess the nodes' locations [6]; for example, this paper uses SG tools to model the surviving BSs' spatial distribution (and also the users' distribution when computing the average coverage probability). Several works have tackled the problem of connectivity in post-disaster scenarios by using SG.

The main literature branch relates to the SG-based performance analysis of UAV-aided post-disaster cellular networks [7]–[9]. In particular, in [7] we used the binomial point process (BPP) and the inhomogeneous Poisson point process (IPPP) to model the post-disaster cellular network, and proposed a novel indicator-function-based SG approach for coverage analysis[1]; then, we extracted useful insights about the coverage probability depending on the type and cardinality of the ad hoc UAV fleet, disaster radius, user's location, and terrestrial network's quality of resilience (QoR). The study proposed in [8], instead, extended the common Matérn and Thomas Poisson cluster processes (PCPs) to capture also the randomness of the coverage holes' sizes, where coverage holes originate from base stations' (BSs') failures; closed-form expressions of the downlink (DL) coverage probability as well as the spectral and energy efficiencies were also provided. Finally, authors in [9] assumed a coexistence of vertical heterogeneous networks (VHetNets) and device-to-device (D2D) communications when studying various uplink performance metrics (namely, energy efficiency, average sum-rate, and probability of successful transmission), and optimized the flight altitude to maximize the energy efficiency.

[1]In fact, compared to conventional methods (such as the ones used in [10], [11]) where the Euclidean plane is subdivided into multiple regions depending also on the user's location, the approach presented in [7] significantly improves the tractability of inhomogeneous system setups with any discontinuity in the expression of the BSs' density.

The second main branch relates to SG modeling of D2D networks for PDCs [12]–[14]. In [12], the authors considered both uplink and downlink connections, and introduced a novel analytical framework to evaluate the effect of a calamity on the network's coverage. The authors investigated how device-to-device (D2D) communications could be used to extend the coverage originating from healthy cells, and provided a comparison between the random BS phase-out and concentrated phase-out scenarios. Moreover, authors in [13] jointly optimized the fraction of spectrum allocated to D2D communications and the small BSs' power and density in order to maximize the system throughput in emergency scenarios. Finally, the authors of [14] used marked Poisson point processes in order to model the aggregate interference and SINR distribution in D2D-aided networks in inband overlay mode.

2) BS Silencing: The idea of BS silencing consists in strategically putting in stand-by some BSs in order to decrease the value of the aggregate interference in some particular zones of the network; in this paper, indeed, silencing will be implemented in order to support disaster-struck regions, as they generally host high-priority users.

The BS silencing practice is well known in the literature: for example, it is often mentioned in the context of green communications, where due to the lack of harvested energy during off-peak hours (for example at night, in case of solar-powered BSs), telecom operators may prefer or even need to switch off some lightly-loaded BSs [15]. Contextually, authors in [16] jointly applied SG and dynamic programming to obtain both optimal and suboptimal BS silencing policies. The study presented in [17], instead, considered heterogeneous networks (HetNets) consisting of both macro and small cell BSs, as well as private femtocell access points (FAPs). In particular, the authors proposed a BS silencing strategy to jointly improve radio resource and power management, and also devised a framework for cooperation agreements between mobile operators and private FAPs.

In the context of non-orthogonal multiple access (NOMA) for cloud radio access networks (RANs), a low complexity algorithm was proposed in [18]: the author devised a greedy heuristic search algorithm that allows to reduce the inter-cell interference by properly assigning the available radio resources. The SG-based framework presented in [19] considered silencing together with other BS cooperation techniques such as joint transmission and the use of Alamouti space-time coding. The obtained results showed that cooperation techniques such as silencing and joint transmission are indeed more effective in case of interference-limited scenarios (low-coverage regime).

Another form of silencing in cooperation schemes regards dynamic point blanking (DPB), sometimes referred to as inter-cell interference coordination (ICIC), where the dominant interferers in the cooperation set are silenced based on the received power (averaged over the fading) [20]. Contextually, authors in [21] derived explicit analytical expressions of the coverage probability in PPP-distributed cellular networks with DPB and intra-cell diversity (ICD). Moreover, [20] studied the meta distribution in DL Poisson HetNets with multiple types of coordinated multipoint (CoMP) schemes, including the ones based on DPB and its combination with dynamic point selection (DPS), according to which the serving BS of any cooperation set is selected as the one with the best instantaneous channel condition.

B. Contributions

The main contributions of this study can be listed as follows:

1) System Model: We consider a large-scale post-disaster wireless network characterized by the resulting density of active BSs. Firstly, we introduce an inhomogeneous PPP (IPPP) to describe the planar distribution of said BSs, and then we propose to silence the ones residing within a certain range of distances from the disaster epicenter.

The entity of the disaster itself is captured by the length of the disaster radius as well as the QoR of the BSs, and the performance of the network (either with or without silencing any BSs) generally depends on these two parameters.

2) Performance Analysis: In this work, we propose a novel SG-based framework which can be used to model realistic post-disaster networks where BS silencing is implemented. In particular, we derive the expressions for the distance distribution to the two nearest BSs and the Laplace transform of the interference in order to compute both the average coverage probability and the SINR meta distribution, which are critical performance metrics to consider in the context of emergency scenarios. Furthermore, to the best of our knowledge this is the first literature work deriving the dominant-interferer-based approximation of the SINR meta distribution for any wireless network modeled as an IPPP, as well as the first paper analyzing the SINR meta distribution (in general) in the context of post-disaster large-scale wireless networks.

The generality of our framework allows to capture important topological aspects such as the size of the disaster radius, the QoR of the terrestrial network, the location of the typical user, and the dimensions of the silencing area (which can be adjusted to provide optimal coverage to

the users inside the disaster area without compromising the coverage within the silencing area itself).

3) System-Level Insights: Another important contribution of this work is represented by the fruitful insights extracted by inspection of the numerical results. For example, depending on the values of the considered parameters, our analytical and simulation results consistently show that there are cases where the user equipment's (UE's) location strongly influences the SINR meta distribution (and hence, the reliability) of the wireless links inside the disaster area, whereas in other cases the reliability almost only depends on whether silencing is applied or not.

Contextually, the trade-off between offering a strong desired signal and causing considerable interference to the UE is punctually explained and further considerations are made for guiding dynamic network planning in emergency situations.

II. System Model

A. Network Model

We consider a disaster-struck cellular network infrastructure. Without affecting the generality of our framework, we set the origin $\boldsymbol{O}$ at the disaster epicenter. The disaster area is modeled as a circle of radius r_d and can expressed as $\mathcal{A}_d = \mathbf{b}(\boldsymbol{O}, r_d) \subset \mathbb{R}^2$, where $\mathbb{R}^2$ denotes the Euclidean ground plane.

We model the distribution of the surviving BSs as an inhomogeneous Poisson point process (IPPP) $\Phi_S \equiv \{W_i\} \subseteq \mathbb{R}^2$ of density $\lambda_S(r) = \lambda_0 \left(\chi(r)\, \mathbb{1}(r \leq r_d) + \mathbb{1}(r > r_d)\right)$, where λ_0 denotes the original BSs' density, r represents the horizontal distance from the origin, and $\chi(r) \in [0, 1]$ is the QoR of the terrestrial infrastructure.

Then, we propose to mitigate the interference inside $\mathcal{A}_d$ by turning off all the BSs that fall within a ring with inner radius r_a and outer radius r_b, with $r_d \leq r_a \leq r_b$. The resulting IPPP and its density can be therefore expressed as $\Phi_T \equiv \{W_i\} \subseteq \Phi_S$ and $\lambda_T(r) = \lambda_S(r) \left(1 - \mathbb{1}(r_a \leq r \leq r_b)\right)$, respectively.

Fig. 1 schematically represents our network model.

B. Channel Model

We introduce Q_{W_i} and Q_{W^*} as the random received powers coming from any generic BS located at point W_i and the closest BS located at W^*, respectively. Furthermore, we assume that the transmitted signals have a fixed and constant power ρ, which attenuates according

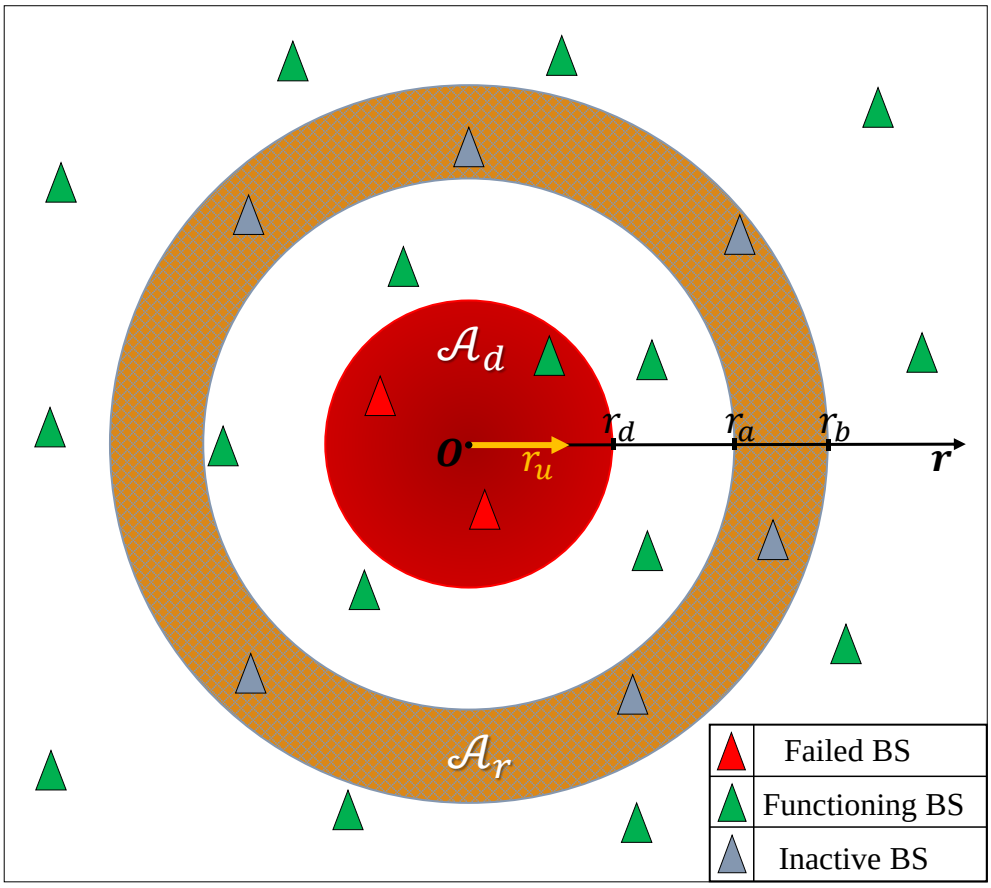

Fig. 1. Qualitative system setup: the typical user has a distance r_u from the epicenter of the disaster (*i.e.*, the origin) and is served by the closest BS, since (on average) it provides maximum received power. All the failed BSs belong to a circular disaster-struck region $\mathcal{A}_d$, whereas the ones turned off are located in a ring $\mathcal{A}_r$ with inner and outer radii r_a and r_b, respectively.

to the standard power-law path loss propagation model with exponent $\alpha > 2$. In addition, random channel effects are modeled as unit-mean exponentially distributed Rayleigh fading gains (denoted by G_{W_i} for any signal coming from a BS located at a generic point W_i, and G_{W^*} for the desired signal). Let η denote the mean loss coefficient (or mean additional losses), then we can define $\xi = \eta\,\rho$. Keeping in mind that BSs are assumed to have negligible altitude (that is, their ground distances from the UE Ω_{W_i}'s coincide with the respective Euclidean distances), we can generally express the standard power-law path-loss as $L(\omega) = \eta\,\omega^{\alpha}$.

The random power received by the typical user from a generic BS can be expressed as

$$Q_{W_i} = \xi\, G_{W_i}\,(1 + \Omega_{W_i})^{-\alpha} \approx \xi\, G_{W_i}\,\Omega_{W_i}^{-\alpha}, \tag{1}$$

where the equality assumes a *modified* path loss to formally avoid the absurdity $Q_{W_i} > \xi$,

occurring for $\Omega_{W_i} < 1\,\mathrm{m}$ (nonetheless, when considering large scale networks, the above approximation is commonly accepted in the literature).

C. Association Policy

In this paper, we adopt the maximum average received power association rule, meaning that the user connects to the BS providing the strongest average received power. Since there is only one tier of BSs, this association policy will make the user associate always with the closest BS. However, this does not imply that there would be no interferers providing higher instantaneous received powers. Finally, we assume a unit mean for the fading gains.

D. SINR

Assuming the serving BS to be located at W^*, the expression of the instantaneous SINR will be

$$\mathrm{SINR} = \frac{Q_{W^*}}{\sigma_n^2 + I}\,, \tag{2}$$

where σ_n^2 and $I = \sum_{\substack{W_i \in \Phi_T \\ W_i \neq W^*}} Q_{W_i}$ denote the powers of the additive white Gaussian noise (AWGN) and aggregate interference, respectively.

E. Coverage Probability

The coverage probability denotes the SINR's complementary cumulative distribution function (CCDF) evaluated at a given threshold $\theta > 0$ that ensures reliable decoding, and is mathematically defined as

$$P_c = \mathbb{P}(\mathrm{SINR} > \theta). \tag{3}$$

F. SINR Meta Distribution

The SINR meta distribution can be defined as the CCDF of the coverage probability (conditioned on the PPP Φ_T) evaluated at a given value of reliability $\gamma \in [0, 1]$, that is

$$\bar{F}_{P_c}(\gamma) = \mathbb{P}\big(\mathbb{P}(\mathrm{SINR} > \theta | \Phi_T) > \gamma\big). \tag{4}$$

III. Performance Analysis

In this section, we derive the distribution of the distance to the closest BS and the conditional Laplace transforms of the interference in order to obtain the expressions of the coverage probability and the SINR meta distribution. Henceforth, wherever not specified, we will assume that the distance r_u between the UE and the disaster epicenter is given.

A. Distance Distributions

In this subsection, we firstly introduce the general distribution of the number of nodes residing within a given distance from the user. Then, we will use this expression to derive the distribution of the distance to the serving BS (Z_0), which is needed to compute the coverage probability. Also, two other distance distributions (to the closest interferer and to the tagged BS conditioned on the distance to the nearest interferer) will be derived, as they will be used later on to conveniently approximate the SINR meta distribution.

Lemma 1. *According to [22], in a two-dimensional HPPP with density λ, the probability of finding k nodes within a distance z can be expressed as*

$$\mathbb{P}[k \text{ HPPP nodes within a distance } z] = \frac{(\pi\, z^2\, \lambda)^k}{k!}\, e^{-\pi z^2 \lambda}. \tag{5}$$

Due to the independence between the points of the PPP, this expression can be easily adapted to the inhomogeneous case, that is

$$\mathbb{P}[k \text{ IPPP nodes within a distance } z] = \frac{\tilde{\mathcal{Y}}(z)}{k!}\, e^{\tilde{\mathcal{Y}}(z)}. \tag{6}$$

where $\tilde{\mathcal{Y}}(z) = \int_0^z \int_0^{2\pi} \tilde{\lambda}(\omega, \beta)\, \omega\, \mathrm{d}\beta\, \mathrm{d}\omega$ and $\tilde{\lambda}(\omega, \beta)$ represents the density of the IPPP.

Having introduced the general formula for the IPPP case, in what follows we will specify it for $k = 1$ and $k = 2$ in order to obtain the distribution to the closest and the second closest BSs, respectively.

Theorem 1. *For a given distance r_u between the typical user and the epicenter of a circular disaster with radius r_d, let $\mathcal{Y}(z) = \int_0^z \int_0^{2\pi} \lambda_T\big(r_\Omega(\omega, \beta)\big)\, \omega\, \mathrm{d}\beta\, \mathrm{d}\omega$, with $r_\Omega(\omega, \beta) = \sqrt{r_u^2 + \omega^2 - 2\, r_u\, \omega\, \cos\beta}$*

being the distance[2] *from the origin. Now, the CDF of the random variable (RV)* Z_0 *denoting the distance between the UE and the closest surviving BS is given by*

$$F_{Z_0}(z) = 1 - e^{-\mathcal{Y}(z)}. \tag{7}$$

Proof: See Appendix A. ■

Corollary 1. *Henceforth, let the overline characterize the complementary functions (i.e.,* $\bar{F}_\Gamma(\gamma) = 1 - F_\Gamma(\gamma)$*). The PDF of the random distance* Z_0 *of the closest functioning BS is*

$$f_{Z_0}(z) = \bar{F}_{Z_0}(z)\, \mathcal{Y}'(z)\,, \tag{8}$$

where $\mathcal{Y}'(z) = \frac{\mathrm{d}\mathcal{Y}(z)}{\mathrm{d}z} = z \int_0^{2\pi} \lambda_T\big(r_\Omega(z,\beta)\big)\, \mathrm{d}\beta$.

Proof: The proof follows by simply computing the derivative of $F_{Z_0}(z)$. More details are provided in Appendix B. ■

Theorem 2. *The CDF of the random distance* Z_1 *of the second closest functioning BS can be expressed as*

$$F_{Z_1}(z) = F_{Z_0}(z)\, \big(1 + \mathcal{Y}(z)\big). \tag{9}$$

Proof: This theorem can be proved by summing the probabilities referring to $k < 2$ from (6). ■

Corollary 2. *The PDF of the distance* Z_1 *between the UE and the second closest functioning BS is*

$$f_{Z_1}(z) = f_{Z_0}(z)\, \big(1 + \mathcal{Y}(z)\big) - \bar{F}_{Z_0}(z)\, \mathcal{Y}'(z). \tag{10}$$

Proof: This corollary can be proven by applying the Leibniz integral rule to $F_{Z_1}(z)$. ■

Now that we have the expressions for the distance distributions of the two closest BSs, we will compute the distributions of each distance conditioned on the other one.

Theorem 3. *The conditional CDF of* Z_1 *(conditioned on* Z_0*) can be expressed as*

$$F_{Z_1|Z_0}(z_1|z_0) = 1 - e^{-\dot{\mathcal{Y}}(z_1|z_0)}, \tag{11}$$

[2] From now on, whenever not specified, we will implicitly refer all the distances to the location of typical UE.

where $\dot{\mathcal{Y}}(z_1|z_0) = \int\limits_{z_0}^{z_1}\int\limits_{0}^{2\pi} \lambda_T\big(r_\Omega(\omega,\beta)\big)\,\omega\,\mathrm{d}\beta\,\mathrm{d}\omega$.

Proof: The proof of this theorem follows from the void probability within the distances (from the user) of the tagged BS and the dominant interferer. ■

Corollary 3. *The PDF of Z_1 conditioned on Z_0 can be expressed as*

$$f_{Z_1|Z_0}(z_1|z_0) = e^{-\dot{\mathcal{Y}}(z_1|z_0)}\,\mathcal{Y}'(z_1). \tag{12}$$

Proof: The conditional PDF $f_{Z_1|Z_0}(z_1|z_0)$ can be obtained as the derivative of its respective CDF. ■

Corollary 4. *Having derived the marginal PDF of the distance to the serving BS and the conditional PDF of the distance to the closest interferer, the joint PDF of Z_0 and Z_1 can be computed as their product:*

$$f_{Z_0,Z_1}(z_0,z_1) = f_{Z_1|Z_0}(z_1|z_0)\,f_{Z_0}(z_0). \tag{13}$$

Corollary 5. *The conditional CDF of Z_0 given Z_1 can be obtained by integrating the respective PDF, that is*

$$F_{Z_0|Z_1}(z_0|z_1) = \int\limits_{0}^{z_0} f_{Z_0|Z_1}(\omega_0,z_1)\,\mathrm{d}\omega_0, \tag{14}$$

where $f_{Z_0|Z_1}(z_0|z_1) = \frac{f_{Z_0,Z_1}(z_0,z_1)}{f_{Z_1}(z_1)}$.

B. Laplace Transform of the Interference

Assuming al BSs to share the same frequency/time resource blocks with reuse factor equal to 1, it follows that co-channel interference is generated by each BS except the tagged one. Therefore, the Laplace transform of the random aggregate interference can be useful to characterize the interference statistics.

Theorem 4. *The Laplace transform of the interference can be expressed as*

$$\mathcal{L}_I(s,z) = \exp\bigg(-\int\limits_{0}^{2\pi}\int\limits_{z}^{\infty} \lambda_T\big(r_\Omega(\tilde{\omega},\beta)\big)\,\mathcal{I}(s,\tilde{\omega})\,\tilde{\omega}\,\mathrm{d}\tilde{\omega}\,\mathrm{d}\beta\bigg), \tag{15}$$

where $\mathcal{I}(s,\omega) = 1 - \Big(\frac{m}{m+\xi\,s\,\omega^{-\alpha}}\Big)^m$.

Proof: See Appendix C. ■

C. Coverage Probability

Now that the expression of the PDF of the distance to the nearest BS and the Laplace transform of the interference are available, we proceed by deriving the coverage probability.

Theorem 5. *Recalling the expressions of $f_{Z_0}(z)$ and $\mathcal{L}_I(s,z)$ respectively provided in Corollary 1 and Theorem 4, the coverage probability experienced by the typical UE is given as*

$$P_c = \int_0^\infty \mathcal{L}_J\big(\mu(z), z\big)\, f_{Z_0}(z)\, \mathrm{d}z\,, \tag{16}$$

where $\mathcal{L}_J(s,z) = e^{-s\,\sigma_n^2}\,\mathcal{L}_I(s,z)$ and $\mu(z) = \frac{m\,\theta}{\xi}\,z^\alpha$.

Proof: See Appendix D. ∎

This, however, allows to compute the coverage probability at a given distance from the disaster epicenter. The following theorem provides the expressions of the average coverage over the two areas of interest, namely the disaster-struck area and the silencing ring.

Theorem 6. *The expected value of the coverage probability over the disaster area $\mathcal{A}_d$ is*

$$\hat{P}_{c,d} = \int_0^\infty \int_0^{r_d} p_c(z)\, f_{Z_0}(z)\, f_{R_u,d}(r)\, \mathrm{d}r\, \mathrm{d}z, \tag{17}$$

whereas the average coverage probability inside the ring hosting the inactive BSs is given by

$$\hat{P}_{c,r} = \int_0^\infty \int_{r_a}^{r_b} p_c(z)\, f_{Z_0}(z)\, f_{R_u,r}(r)\, \mathrm{d}r\, \mathrm{d}z, \tag{18}$$

where, in case of uniformly distributed users, $f_{R_u,d}(r) = \frac{2r}{r_d^2}$ and $f_{R_u,r}(r) = \frac{2r}{(r_b^2 - r_a^2)}$.

Proof: The results follow from the integration of the coverage probability over the PDF of the RV R_u specified for the area of interest.

However, another approach to compute $\hat{P}_{c,d}$ (and, similarly, also $\hat{P}_{c,r}$) is the following:

$$\hat{P}_{c,d} = \frac{2\pi \int_0^{r_d}\int_0^\infty p_c(z)\, f_{Z_0}(z)\, \lambda_u(r)\, r\, \mathrm{d}z\, \mathrm{d}r}{2\pi \int_0^{r_d} \lambda_u(r)\, r\, \mathrm{d}r} = \frac{\int_0^{r_d}\int_0^\infty p_c(z)\, f_{Z_0}(z)\, \lambda_u(r)\, r\, \mathrm{d}z\, \mathrm{d}r}{\int_0^{r_d} \lambda_u(r)\, r\, \mathrm{d}r}\,, \tag{19}$$

where $\lambda_u(r)$ describes the density of users as a function of the distance from the disaster epicenter; in case of uniform distribution the expression becomes

$$\hat{P}_{c,d} = \frac{2\,\lambda_u \int_0^{r_d}\int_0^\infty p_c(z)\, f_{Z_0}(z)\, r\, \mathrm{d}z\, \mathrm{d}r}{\lambda_u\, r_d^2} = \frac{2}{r_d^2}\int_0^\infty \int_0^{r_d} p_c(z)\, f_{Z_0}(z)\, r\, \mathrm{d}r\, \mathrm{d}z, \tag{20}$$

which is indeed equivalent to (17) when $f_{R_u,d}(r) = \frac{2r}{r_d^2}$. ∎

D. SINR Meta Distribution

In this subsection, we provide the exact and approximated expressions of the SINR meta distribution.

Theorem 7. *The exact expression of the SINR meta distribution is [23]*

$$\bar{F}_{P_c}(\gamma) = \frac{1}{2} + \frac{1}{\pi} \int_0^\infty \frac{\mathrm{Im}\big(e^{-jt \log \gamma}\, \mathcal{M}_{jt}\big)}{t}\, \mathrm{d}t, \tag{21}$$

where the operator $\mathrm{Im}(\zeta)$ *denotes the imaginary part of* $\zeta \in \mathbb{C}$*, and* $\mathcal{M}_b = \int_0^\infty p_c^b(z)\, f_{Z_0}(z)\, \mathrm{d}z$ *represents the* b*-th moment of the SINR meta distribution.*

Proof: See Appendix E. ■

Given the complexity of the exact expression of SINR meta distribution, we hereby derive a useful (yet accurate) approximation by recalling the expressions of the PDF of Z_1 and the CDF of Z_0 conditioned on Z_1.

Theorem 8. *Let* $v(z) = \theta\left(\mathcal{G}(z) + \frac{\sigma_n^2}{\xi}\right)$*, with* $\mathcal{G}(z) = \int_z^\infty \int_0^{2\pi} \lambda_T\big((r_\Omega(\omega,\beta)\big)\, \omega^{-\alpha+1}\, \mathrm{d}\beta\, \mathrm{d}\omega$*. By recalling the expressions of* $f_{Z_1}(z_1)$ *from Corollary 2 and* $F_{Z_0|Z_1}(z_0|z_1)$ *from Corollary 5, the dominant-interferer-based approximation of the SINR meta distribution [24] can be computed as*

$$\bar{F}_{P_c}(\gamma) \approx \int_0^\infty F_{Z_0|Z_1}\Big(\min\big(\mathcal{K}(z), z\big)\big|z\Big)\, f_{Z_1}(z)\, \mathrm{d}z, \tag{22}$$

where

$$\mathcal{K}(z) = \sqrt[\alpha]{\max\left(0, -\frac{z^\alpha}{\theta} + \frac{1}{v(z)}\, \mathcal{W}_0\left(\frac{v(z)\, z^\alpha\, e^{\frac{v(z)\, z^\alpha}{\theta}}}{\gamma\, \theta}\right)\right)} \tag{23}$$

with $\mathcal{W}_0(w)$ *denoting the principal branch of the Lambert function, which is defined as* $\mathcal{W}(w)\, e^{\mathcal{W}(w)} = w$*.*

Proof: See Appendix F. ■

IV. Results and Discussion

In this section, we show insightful simulation and analytical results (represented as lines and markers, respectively) based on performance metrics such as the average coverage probability and the SINR meta distribution. To this extent, we make use of Monte Carlo simulations and verify

TABLE I

MAIN SYSTEM PARAMETERS' STANDARD VALUES

Parameters	**Values**
Original BSs' density	$\lambda_0 = 2\,\text{BSs/km}^2 = 2\times10^{-6}\,\text{BSs/m}^2$
Path loss exponent	$\alpha = 3$
BSs' transmit power	$\rho = 20\,\text{W}$
SINR threshold	$\theta = -7\,\text{dB} = 0.2$
Noise power	$\sigma_n^2 = 10^{-11}\,\text{W}$
Average coverage priority ratio (introduced in Sec. IV-A)	$\tau = 3$

them analytically by applying the expressions derived in Sec. III. Then, we will try to extract useful information about the influence of various parameters (such as the QoR χ, disaster radius r_d, and distance from the epicenter r_u[3]) by inspection of the proposed plots. In fact, the observed trends can be helpful in disaster management practices: for example, by predicting or estimating the entity of the specific calamity, the network operator would be able to quantify the advantages of strengthening the terrestrial infrastructure or silencing a specific region, respectively.

It should be taken into account that BSs present limitations in terms of capacity (hence the network may suffer from overload when silencing is applied to some nodes), which considerations are beyond the scope of this study. Finally note that, unless stated otherwise, the network parameters are set according to Table I.

A. Average Coverage Probability

In this subsection, we optimize the silencing ring's radii r_a and r_b so that the average coverage probability within the disaster area ($\hat{P}_{c,d}$) is maximized without excessively reducing the average coverage probability inside the ring before silencing any BSs ($\hat{P}_{c,r_0}$). In other words, our goal is

[3] While varying these parameters, we fix the original BS density λ_0 since we expect the network to be interference-limited; hence, if λ_0 increases then the interference increases and the distance to the tagged BS decreases in such a way that the SINR remains almost constant [25].

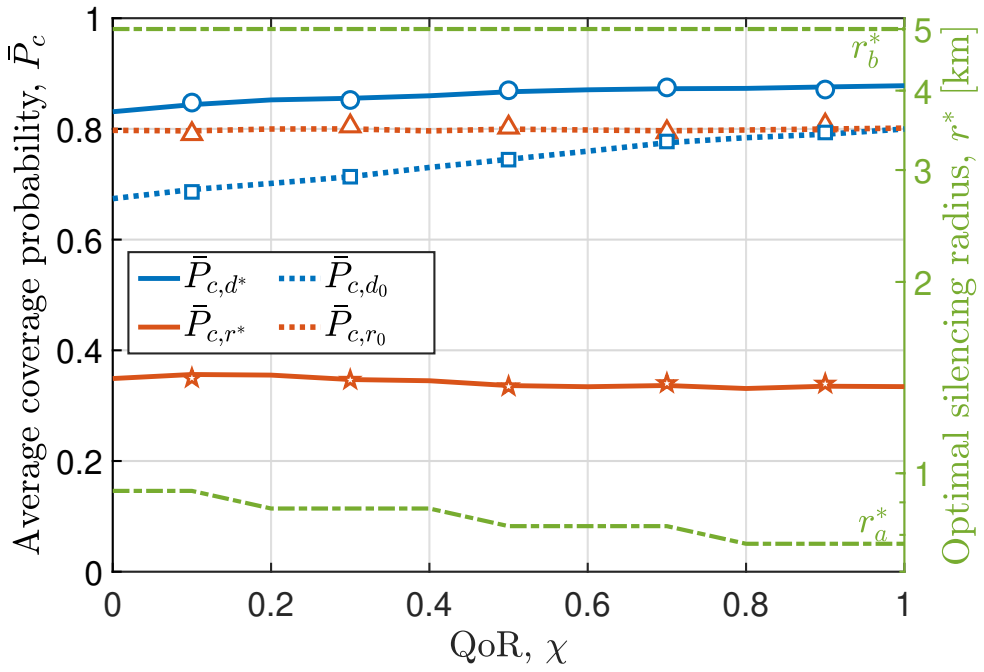

(a)

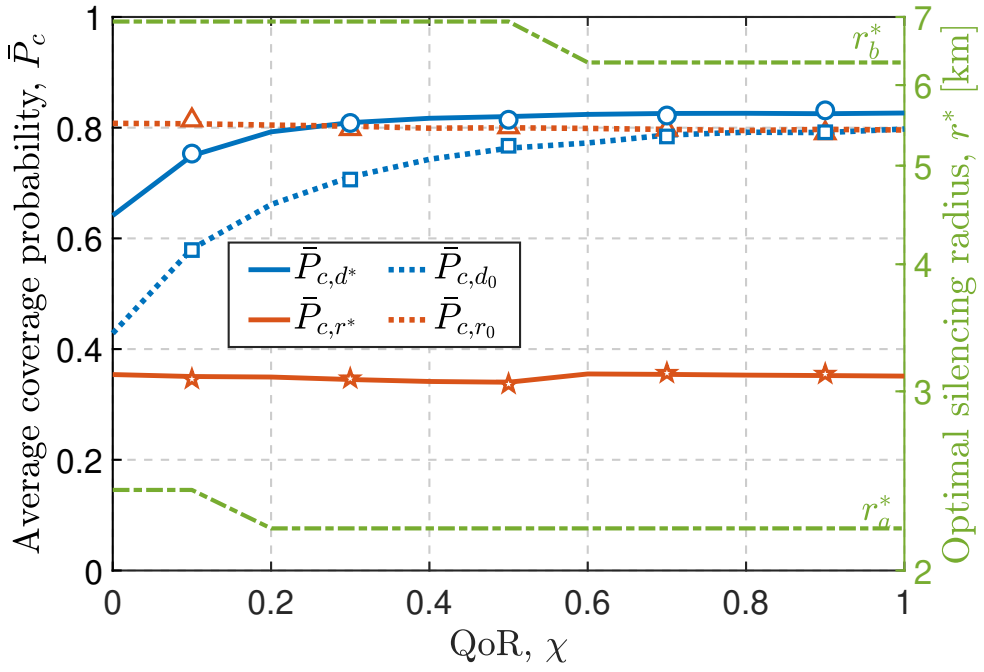

(b)

Fig. 2. Average coverage probabilities over $\mathcal{A}_d$ and $\mathcal{A}_r$, with and without the proposed silencing strategy, as function of the QoR when: (a) $r_d = 500\,\text{m}$ and (b) $r_d = 2\,\text{km}$. The respective optimal silencing radii (obtained by exhaustive search with Monte Carlo simulations) are also plotted with respect to the y-axes on the right side of the figures.

to find the best values of r_a and r_b (say, r_a^* and r_b^*) meeting the following optimization statement:

$$\begin{aligned} &\underset{r_a, r_b}{\text{maximize}} \;\; \hat{P}_{c,d} \\ &\text{subject to} \;\; \hat{P}_{c,r} > \frac{\hat{P}_{c,r_0}}{\tau}\,, \end{aligned} \tag{24}$$

where $\hat{P}_{c,r}$ is the average value of the coverage probability inside $\mathcal{A}_r$ and the *average coverage priority ratio* $\tau > 1$ is a constant introduced to set the maximum cost (in terms of reduction of the average coverage inside the ring) allowed for the proposed interference mitigation strategy.

To avoid affecting an excessive number of users, we limit the outer radius of the silencing ring to a maximum of ten times the disaster radius, that is, $r_b \leq 10 r_d$. Then, we consider two different values of the disaster radius (namely $r_d = 500\,\text{m}$ and $r_d = 2\,\text{km}$) and proceed with an exhaustive search of r_a^* and r_b^* in order to compare the average coverage probabilities in case of optimal silencing (denoted as $\hat{P}_{c,d^*}$ and $\hat{P}_{c,r^*}$) with the ones in case of no silencing (denoted as $\hat{P}_{c,d_0}$ and $\hat{P}_{c,r_0}$), as functions of the QoR χ; it is worth noting that the considered values of r_d refer only to small- and medium-size disasters, as the proposed strategy is not recommended for large-size disasters because of the large path-loss exponent characterizing terrestrial communications (which in turn would make silencing ineffective if the typical user is nearby the disaster epicenter). Trivially, we can anticipate that the original values of the average coverage probabilities inside $\mathcal{A}_d$ and $\mathcal{A}_r$ in case of fully-resilient networks (for which $\chi = 1$) should coincide, as the system setup essentially boils down to a homogeneous Poisson network.

1) Small-Size Disasters: When r_d equals half a kilometer, we can see from Fig. 2-a that r_b^* is always maximum, while r_a^* slightly decreases as χ increases because a more resilient network allows to better support also the users located at the inner edge of $\mathcal{A}_r$. On the other side, both $\hat{P}_{c,r_0}$ and the resulting value of the average coverage inside the ring ($\hat{P}_{c,r^*}$) are almost constant with respect to χ.

Recalling that $\tau = 3$, we can note that the cost of this interference mitigation approach roughly equals to 45 percentage points on $\hat{P}_{c,r}$, and can be justified only by the higher priority of the users located inside $\mathcal{A}_d$; in particular, for the worst case scenario ($\chi \to 0$), by optimizing the silencing radii we can boost $\bar{P}_{c,d}$ from just 67.4% to 83.1%.

Evidently, in the absence of any disaster this strategy would be extremely inconvenient since there is no priority for the respective users, although the improvement in terms of $\bar{P}_{c,d}$ (that is, the average coverage within the same area $\mathcal{A}_d$) would still be substantial.

2) Medium-Size Disasters: For the case with $r_d = 2\,\text{km}$, we can infer from Fig. 2b that r_b^* equals to roughly one-third of its maximum value of $20\,\text{km}$, and may slightly decrease in case of more resilient networks (similarly to r_a*). While the average difference between $\hat{P}_{c,r_0}$ and $\hat{P}_{c,r^*}$ is very similar to the one noted for small-size disasters, decreasing r_b^* when χ exceeds 0.5 slightly enhances $\hat{P}_{c,r}$.

When χ is small, the relatively large value of r_d compromises $\hat{P}_{c,d_0}$ and therefore silencing becomes vital for the users inside $\mathcal{A}_d$: the plot indeed shows that $\hat{P}_{c,d^*} - \hat{P}_{c,d_0} \approx 0.22$ at $\chi = 0$. On the other hand, as χ increases the benefit of silencing becomes less and less evident, amounting to just 0.03 for the case of a fully-resilient network.

B. SINR Meta Distribution

Now, having ensured that the coverage within the silencing ring is not excessively reduced, we can focus on the reliability of the network from the point of view of a typical user located at a given distance $r_u \leq r_d$ (and, due also to space limitations, omit the case $r_a^* < r_u < r_b^*$, since the typical user would have a lower priority). To do this, we consider again r_d equal to either 500 or $2000\,\text{m}$ (assuming specific values of the QoR and extracting the corresponding values of r_a^* and r_b^* from Figs. 2-a and 2-b), and evaluate the SINR meta distribution as a function of the reliability of the wireless links.

1) Non-Resilient Networks: The behaviors of the SINR meta distributions in case of non-resilient networks where r_d equals to either half or two kilometers can be respectively observed in Figs. 3-a and 3-b. In particular, by comparing the two plots we can strongly confirm the intuition that a larger disaster radius implies a larger impact of the user's location within $\mathcal{A}_d$.

From Fig. 3-a, we can see that in the occurrence of a small-sized calamity, the maximum gain brought by the optimal silencing would be achieved at $\gamma \approx 0.7$, ranging from 0.28 to 0.58 as r_u is decreased from r_d to 0. Moreover, we can surprisingly observe that, with optimal silencing, the SINR meta distribution does not depend on r_u unless $\gamma \geq 0.5$: this means that for $r_d = 500\,\text{m}$, even if the network is not resilient at all, the basic level of reliability of the wireless links can still be preserved with silencing. At the same time, however, we should also understand that high quality services (for example $\gamma > 0.8$) become rare in the proximity of the disaster epicenter. Finally, a minor consideration can be made regarding the behaviors of the solid and dotted lines for $\gamma \leq 0.2$, since the user located at distance r_d from the epicenter would surprisingly experience reliable connectivity for a slightly lower percentage of the time,

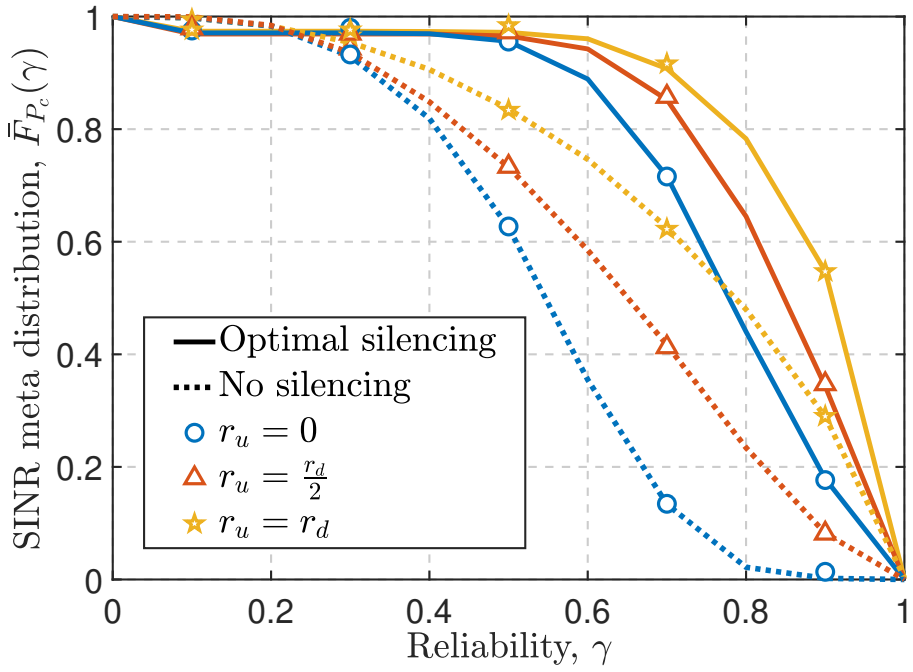

(a)

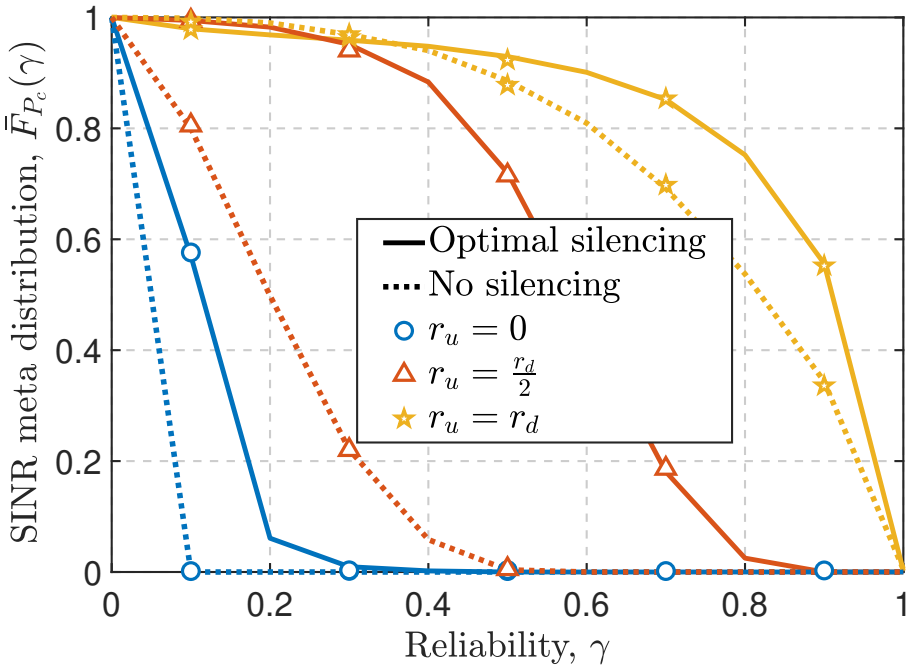

(b)

Fig. 3. SINR meta distribution, for various values of r_u, as function of the links' reliability when $\chi = 0$ and: (a) $r_d = 500\,\mathrm{m}$ and (b) $r_d = 2\,\mathrm{km}$.

compared to another user located at half of the distance; this is because despite the shorter average distance to the serving BS, the effect of a stronger aggregate interference can easily affect the quality of service (QoS).

Fig. 3-b conveys that when $r_d = 2\,\text{km}$ the considered terrestrial network rarely provides coverage for a sufficient percentage of the time (say, $\gamma \geq 0.6$) to the users located nearby the disaster epicenter (see the blue curves, corresponding to $r_u = 0$). In particular, the users located at the epicenter of the disaster would not be able to enjoy any real-time connectivity at all, but could still communicate by making use of low-bandwidth and delay-tolerant services such as text messages.

2) Partially-Resilient Networks: By increasing χ to 0.5, we can see from Figs. 4-a and 4-b that the SINR meta distribution in partially-resilient networks becomes almost independent from the location of the typical user.

Nonetheless, in case of small disasters (Fig. 4-a), optimal silencing would still be very effective: assuming a uniform distribution of the users, sufficient reliability (that is, $\gamma \geq 0.6$) would be achieved by roughly 97% of them (instead of just 78% for the case without silencing). However, again, we can observe that the proposed silencing strategy is slightly detrimental for $\gamma \to 0$.

For the case with $r_d = 2\,\text{km}$, instead, Fig. 4-b conveys that the benefit of implementing optimal silencing is much more limited, but still evident. Finally, it is interesting to note from the dotted curves that, before silencing, the SINR meta distribution at the disaster epicenter is always (slightly) higher than the one kilometer of distance; in fact, compared to a user located at $r_u = 1\,\text{km}$, a user at the disaster epicenter would have the almost same average distance to the serving BS, but its SINR would be higher because of the lower density of nearby interferers.

V. Summary and Future Works

This paper introduced a novel, concise, and tractable SG framework specifically designed to estimate the QoS in silencing-enabled terrestrial post-disaster cellular networks. In particular, the proposed model includes analytical expressions for the distance distributions to the two closest BSs and the Laplace transform of the interference, which are needed to derive the exact expressions of average coverage probabilities as well as the exact and approximate expressions of the SINR meta distribution experienced by a typical UE. Furthermore, the consistency between our simulated and analytical results proved that proper BS silencing can be a key-enabler for

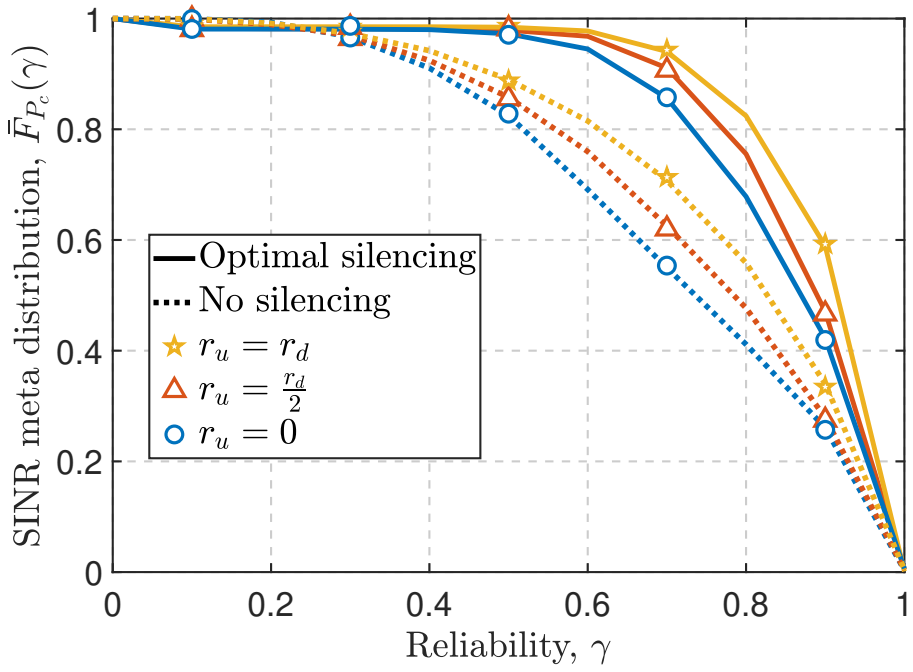

(a)

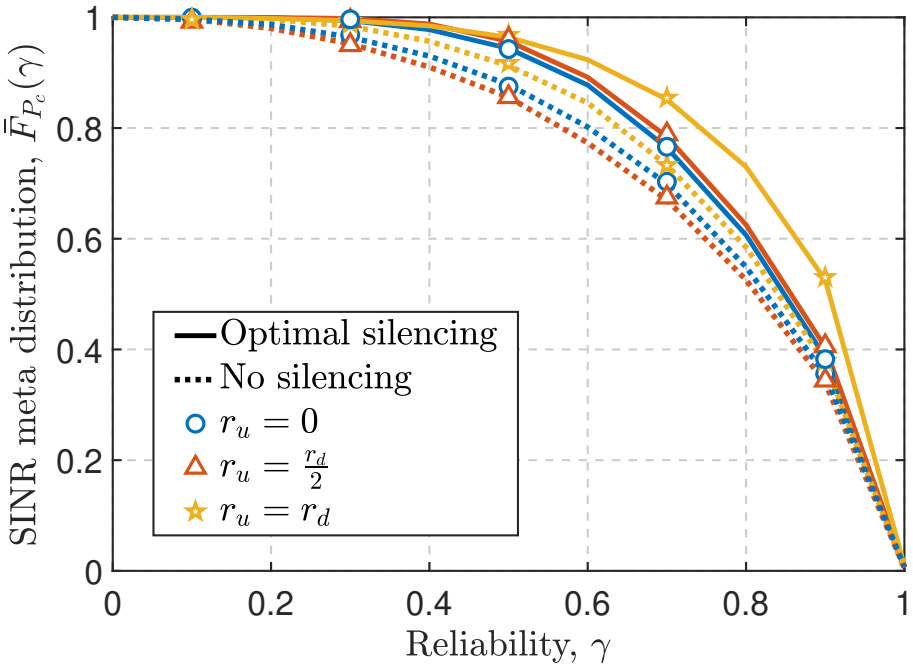

(b)

Fig. 4. SINR meta distribution, for various values of r_u, as function of the links' reliability when $\chi = 0.5$ and: (a) $r_d = 500\,\mathrm{m}$ and (b) $r_d = 2\,\mathrm{km}$.

ensuring sufficient level of coverage and reliability in unfortunate circumstances, and allowed us to extract several insights that can be used for improving network management.

This work could be expanded along multiple research directions. For example, it is evident that silencing BSs increases the risk of overloading the network, and therefore it would be important to carry on an accurate load analysis for the proposed setup. Alternatively, a more general setup where the terrestrial infrastructure consists of multiple tiers could be studied later on. Finally, it would also be worth devising proper spectrum allocation schemes that allow to mitigate the interference coming from some of BSs without the need of silencing them.

APPENDIX A
PROOF OF THEOREM 1

The CDF of Z_0 follows from the null probability of the PPP [26]. Let $N_T(z)$ be the number of BSs residing within a distance z from the UE, then:

$$\begin{aligned} F_{Z_0}(z) &= \mathbb{P}(Z_0 \leq z) = 1 - \mathbb{P}(Z_0 > z) = 1 - \mathbb{P}\big(N_T(z) = 0\big) \\ &= 1 - \exp\bigg(- \int_0^{2\pi} \int_0^{z} \lambda_T\big(r_\Omega(\omega, \beta)\big)\, \omega \, \mathrm{d}\omega \, \mathrm{d}\beta \bigg), \end{aligned} \tag{25}$$

where $r_\Omega(\omega, \beta) = \sqrt{r_u^2 + \omega^2 - 2\, r_u\, \omega\, \cos\beta}$ and $\lambda_T\big(r_\Omega(\omega, \beta)\big)$ describe the distance from the origin and the working BSs' density from the user's perspective, respectively.

APPENDIX B
PROOF OF COROLLARY 1

The derivative of $F_{Z_0}(z)$ is

$$f_{Z_0}(z) = - \exp\bigg(- \int_0^{2\pi} \int_0^{z} \lambda_T\big(r_\Omega(\omega, \beta)\big)\, \omega \, \mathrm{d}\omega \, \mathrm{d}\beta \bigg) \times \bigg(- \frac{\mathrm{d}}{\mathrm{d}z} \int_0^{2\pi} \int_0^{z} \lambda_T\big(r_\Omega(\omega, \beta)\big)\, \omega \, \mathrm{d}\omega \, \mathrm{d}\beta \bigg), \tag{26}$$

where, introducing $g_z(z, \beta) = \int_0^{z} \lambda_T\big(r_\Omega(\omega, \beta)\big)\, \omega \, \mathrm{d}\omega$ and applying the Leibniz integral rule, we have

$$\begin{aligned} \frac{\mathrm{d}}{\mathrm{d}z} \int_0^{2\pi} g_z(z, \beta)\, \mathrm{d}\beta &= g_z(z, 2\pi)\, \frac{\mathrm{d}}{\mathrm{d}z}(2\pi) - g_z(z, 0)\, \frac{\mathrm{d}}{\mathrm{d}z}(0) + \int_0^{2\pi} \frac{\partial}{\partial z}\, g_z(z, \beta)\, \mathrm{d}\beta \\ &= 0 - 0 + \int_0^{2\pi} \frac{\mathrm{d}}{\mathrm{d}z} g_z(z, \beta)\, \mathrm{d}\beta = z \int_0^{2\pi} \lambda_T\big(r_\Omega(z, \beta)\big)\, \mathrm{d}\beta\,, \end{aligned} \tag{27}$$

which completes the proof.

APPENDIX C
PROOF OF THEOREM 4

Let $\mathbf{W}$ denote the set of coordinates of the functioning BSs and $\mathcal{I}_T(s,\omega) = 1 - \left(\frac{m}{m+\xi\, s\, \omega^{-\alpha}}\right)^m$. Then, the conditional Laplace transform of the interference can be obtained as follows [27, Eq. (4), (16)]:

$$\begin{aligned}\mathcal{L}_I(s,z) = \mathbb{E}\Big[e^{-s\,I}\Big] &\overset{(a)}{=} \mathbb{E}_{\Phi_T}\Bigg[\prod_{W_i\in\check{\Phi}_T} \psi_T(s,W_i)\Bigg] \\ &\overset{(b)}{=} \exp\Bigg(-\int_{\mathbb{R}^2\setminus\mathcal{B}_z(z)} \lambda_T(\|\mathbf{W}\|)\,\big(1-\psi_T(s,\mathbf{W})\big)\,\mathrm{d}\mathbf{W}\Bigg) \\ &= \exp\Bigg(-\int_0^{2\pi}\int_z^{\infty} \lambda_T\big(r_\Omega(\check{\omega},\beta)\big)\,\mathcal{I}_T(s,\check{\omega})\,\check{\omega}\,\mathrm{d}\check{\omega}\,\mathrm{d}\beta\Bigg), \end{aligned} \tag{28}$$

where $\psi_T(s,W_i) = \mathbb{E}_{G_{W_i}}\left[\exp\left(-\frac{s\,G_{W_i}\,\xi}{\|W_i\|^\alpha}\right)\right]$. Step (a) is due to the fact that the exponentially distributed gains G_{W_i}'s are independent from each other, whereas (b) follows by applying the probability generating functional (PGFL) to $\psi_T(s,W_i)$.

APPENDIX D
PROOF OF THEOREM 5

The mathematical expression of the coverage probability can be obtained as

$$P_c = \mathbb{E}_{Z_0}\big[\mathbb{P}(\mathrm{SINR} > \theta \,|\, Z_0)\big] = \mathbb{E}_{Z_0}\big[p_c(Z_0)\big] = \int_{\mathbb{R}^+} p_c(z)\, f_{Z_0}(z)\,\mathrm{d}z, \tag{29}$$

in which the conditional coverage probability is expressed as

$$p_c(z) = \mathbb{P}\left(\frac{\xi\, G_{W^*}\, z^{-\alpha}}{J} > \theta\right) = \mathbb{P}\left(G_{W^*} > \frac{\theta\, J}{\xi}\, z^\alpha\right) = \mathbb{E}_J\left[\bar{F}_G\left(\frac{\theta\, J}{\xi}\, z^\alpha\right)\right], \tag{30}$$

with $J = \sigma_n^2 + I$. Since the CCDF of the exponential distribution with unit mean is $\bar{F}_G(g) = e^{-g}$, we can introduce $\mu(z) = \frac{\theta}{\xi}\, z^\alpha$ and rewrite

$$p_c(z) = \mathbb{E}_J[e^{-\mu(z)\,J}] = \mathcal{L}_J\big(\mu(z),z\big) = e^{-s\,\sigma_n^2}\,\mathcal{L}_I(s,z), \tag{31}$$

which completes the proof.

APPENDIX E
PROOF OF THEOREM 7

In order to compute the exact expression of the SINR meta distribution, let us first define the b-th moment of the SINR meta distribution as the expected value of the b-th power of the conditional coverage probability:

$$\mathcal{M}_b = \mathbb{E}_{Z_0}\big[p_c^b(Z_0)\big] = \int_0^\infty p_c^b(z)\, f_{Z_0}(z)\,\mathrm{d}z. \tag{32}$$

Now, recalling that the jt-th moment corresponds to the characteristic function of the RV $C = \log p_c(Z)$, we can apply the Gil-Pelaez theorem as in [23, Corollary 3] and obtain

$$\bar{F}_C(c) = \frac{1}{2} + \frac{1}{\pi}\int_0^\infty \frac{\mathrm{Im}(e^{-jt\,c}\,\mathcal{M}_{jt})}{t}\,\mathrm{d}t. \tag{33}$$

Finally, by noting that $\mathbb{P}\big(p_c(Z_0) > c\big) = \mathbb{P}\big(\log p_c(Z_0) > \log c\big)$ we obtain the expression in (21).

APPENDIX F
PROOF OF THEOREM 8

By approximating the aggregate interference as the sum of the interference coming from the closest BSs and the expectation of the aggregate interference due to all the other BSs (*i.e.*, by focusing only on the dominant interferer), the coverage probability becomes:

$$\begin{aligned} P_c &= \mathbb{P}\bigg(\frac{\xi\, G_0\, Z_0^{-\alpha}}{\sum\limits_{i\in\mathbb{N}^+}\xi\, G_i\, Z_i^{-\alpha} + \sigma_n^2} > \theta\bigg) = \mathbb{P}\bigg(G_0 > \theta\, Z_0^\alpha\Big(\sum_{i\in\mathbb{N}^+} G_i\, Z_i^{-\alpha} + \frac{\sigma_n^2}{\xi}\Big)\bigg) \\ &\approx \mathbb{E}_G\bigg[\exp\bigg(-\theta\, Z_0^\alpha\Big(G_1\, Z_1^{-\alpha} + \mathcal{G}(Z_1) + \frac{\sigma_n^2}{\xi}\Big)\bigg)\bigg] = \frac{\exp\big(-v(Z_1)\, Z_0^\alpha\big)}{1+\theta\left(\frac{Z_0}{Z_1}\right)^\alpha}, \end{aligned} \tag{34}$$

where $v(z) = \theta\big(\mathcal{G}(z) + \frac{\sigma_n^2}{\xi}\big)$, with $\mathcal{G}(z) = \int\limits_z^\infty\int\limits_0^{2\pi} \lambda_T\big(r_\Omega(\omega,\beta)\big)\,\omega^{-\alpha}\,\mathrm{d}\beta\,\omega\,\mathrm{d}\omega$ representing the expected value (normalized on the transmit power) of the aggregate interference coming from all non-dominant interferers; note that the expression of $\mathcal{G}(z)$ follows from Campbell's theorem and can be obtained by following the same approach suggested in [27, Example 5].

Then, recalling that $Z_0 < Z_1$, the dominant-interferer-based approximation of the SINR meta distribution can be obtained as [24]

$$\begin{aligned}\bar{F}_{P_c}(\gamma) &= \mathbb{P}(P_c > \gamma) \\ &\approx \mathbb{E}_{Z_1}\left[\mathbb{P}\left(\exp\left(-v(Z_1)\,Z_0^{\alpha}\right) > \gamma + \theta\,\gamma\left(\frac{Z_0}{Z_1}\right)^{\alpha}\Big| Z_1\right)\right] \\ &\overset{(a)}{=} \mathbb{E}_{Z_1}\Big[\mathbb{P}\Big(Z_0 < \mathcal{K}(Z_1)\big|Z_1\Big)\Big] = \mathbb{E}_{Z_1}\big[F_{Z_0|Z_1}\big(\mathcal{K}(Z_1)\big)\big], \end{aligned} \tag{35}$$

where $\mathcal{K}(z) = \mathrm{Re}\left(\sqrt[\alpha]{-\frac{z^{\alpha}}{\theta} + \frac{1}{v(z)}\,\mathcal{W}_0\left(\frac{v(z)\,\exp(\theta^{-1}\,v(z)\,z^{\alpha})}{\theta\,\gamma\,z^{-\alpha}}\right)}\right)$ with $\mathcal{W}_0(w)$ denoting the principal branch of the Lambert function, which in turn is defined as $\mathcal{W}(w)\,e^{\mathcal{W}(w)} = w$. Step (a) can be performed by introducing $\kappa = \theta\,Z_1^{-\alpha}$, solving the respective symbolic equation on MATLAB, and properly simplify the result.

REFERENCES

[1] United Nations Office for Coordination of Humanitarian Affairs (UNOCHA), "The Story of INSARAG 20 Years On..." 2010.

[2] C. Esposito, Z. Zhao, and J. Rak, "Reinforced secure gossiping against DoS attacks in post-disaster scenarios," *IEEE Access*, vol. 8, pp. 178 651–178 669, 2020.

[3] M. Matracia, N. Saeed, M. A. Kishk, and M.-S. Alouini, "Post-disaster communications: Enabling technologies, architectures, and open challenges," *IEEE Open Journal of the Communications Society*, vol. 3, pp. 1177–1205, 2022.

[4] T. Sakano, Z. M. Fadlullah, T. Ngo, H. Nishiyama, M. Nakazawa, F. Adachi, N. Kato, A. Takahara, T. Kumagai, H. Kasahara, and S. Kurihara, "Disaster-resilient networking: a new vision based on movable and deployable resource units," *IEEE Network*, vol. 27, no. 4, pp. 40–46, 2013.

[5] M. Matracia, M. A. Kishk, and M.-S. Alouini, "On the topological aspects of UAV-assisted post-disaster wireless communication networks," *IEEE Communications Magazine*, vol. 59, no. 11, pp. 59–64, 2021.

[6] Y. Hmamouche, M. Benjillali, S. Saoudi, H. Yanikomeroglu, and M. Di Renzo, "New trends in stochastic geometry for wireless networks: A tutorial and survey," *Proceedings of the IEEE*, vol. 109, no. 7, pp. 1200–1252, 2021.

[7] M. Matracia, M. A. Kishk, and M.-S. Alouini, "UAV-aided post-disaster cellular networks: A novel stochastic geometry approach," *IEEE Transactions on Vehicular Technology*, to appear.

[8] A. M. Hayajneh, S. A. R. Zaidi, D. C. McLernon, M. Di Renzo, and M. Ghogho, "Performance analysis of UAV enabled disaster recovery networks: A stochastic geometric framework based on cluster processes," *IEEE Access*, vol. 6, pp. 26 215–26 230, 2018.

[9] M. Rihan, M. M. Selim, C. Xu, and L. Huang, "D2D communication underlaying UAV on multiple bands in disaster area: Stochastic geometry analysis," *IEEE Access*, vol. 7, pp. 156 646–156 658, 2019.

[10] V. V. Chetlur and H. S. Dhillon, "Downlink coverage analysis for a finite 3-D wireless network of unmanned aerial vehicles," *IEEE Transactions on Communications*, vol. 65, no. 10, pp. 4543–4558, 2017.

[11] M. Matracia, M. A. Kishk, and M.-S. Alouini, "Coverage analysis for UAV-assisted cellular networks in rural areas," *IEEE Open Journal of Vehicular Technology*, vol. 2, pp. 194–206, 2021.

[12] A. Al-Hourani, S. Kandeepan, and A. Jamalipour, "Stochastic geometry study on device-to-device communication as a disaster relief solution," *IEEE Transactions on Vehicular Technology*, vol. 65, no. 5, pp. 3005–3017, 2015.

[13] A. Ravichandran, A. Alnoman, N. Sharma, and A. Anpalagan, "Traffic offloading problem in two-tier HetNets with D2D support for emergency communications," in *IEEE Canada International Humanitarian Technology Conference (IHTC)*, Toronto, ON, Canada, 2017, pp. 128–132.

[14] S. Chakrabarti and S. Das, "Poisson point process-based network modelling and performance analysis of multi-hop D2D chain relay formation in heterogeneous wireless network," *International Journal of Communication Networks and Distributed Systems*, vol. 22, no. 1, pp. 98–122, 2019.

[15] F. O. Ehiagwina, O. Kehinde, A. Adewale, O. Seluwa, and J. Anifowose, "An insight into deployments of green base stations (GBSs) for an environmentally sustainable world," in *IOP Conference Series: Materials Science and Engineering*, vol. 1107, no. 1. IOP Publishing, Sanya, Hainan Province, China, 2021, pp. 621–635.

[16] Y. L. Che, L. Duan, and R. Zhang, "Dynamic base station operation in large-scale green cellular networks," *IEEE Journal on Selected Areas in Communications*, vol. 34, no. 12, pp. 3127–3141, 2016.

[17] H. Ghazzai, M. J. Farooq, A. Alsharoa, E. Yaacoub, A. Kadri, and M.-S. Alouini, "Green networking in cellular HetNets: A unified radio resource management framework with base station ON/OFF switching," *IEEE Transactions on Vehicular Technology*, vol. 66, no. 7, pp. 5879–5893, 2016.

[18] R. S. Rai, "Coordinated scheduling for non-orthogonal multiple access (NOMA) in a cloud-RAN system," in *International Conference on Communications (ICC)*. IEEE, Kansas City, MO, USA, 2018, pp. 1–6.

[19] G. Nigam, P. Minero, and M. Haenggi, "Spatiotemporal cooperation in heterogeneous cellular networks," *IEEE Journal on Selected Areas in Communications*, vol. 33, no. 6, pp. 1253–1265, 2015.

[20] Q. Cui, X. Yu, Y. Wang, and M. Haenggi, "The SIR meta distribution in Poisson cellular networks with base station cooperation," *IEEE Transactions on Communications*, vol. 66, no. 3, pp. 1234–1249, 2017.

[21] X. Zhang and M. Haenggi, "A stochastic geometry analysis of inter-cell interference coordination and intra-cell diversity," *IEEE Transactions on Wireless Communications*, vol. 13, no. 12, pp. 6655–6669, 2014.

[22] M. Haenggi, "On distances in uniformly random networks," *IEEE Transactions on Information Theory*, vol. 51, no. 10, pp. 3584–3586, 2005.

[23] ——, "The meta distribution of the SIR in Poisson bipolar and cellular networks," *IEEE Transactions on Wireless Communications*, vol. 15, no. 4, pp. 2577–2589, 2016.

[24] Y. Qin, M. A. Kishk, and M.-S. Alouini, "A dominant interferer plus mean field-based approximation for SINR meta distribution in wireless networks," *IEEE Transactions on Communications*, to appear.

[25] H. S. Dhillon, R. K. Ganti, F. Baccelli, and J. G. Andrews, "Modeling and analysis of K-tier downlink heterogeneous cellular networks," *IEEE Journal on Selected Areas in Communications*, vol. 30, no. 3, pp. 550–560, 2012.

[26] J. G. Andrews, F. Baccelli, and R. K. Ganti, "A tractable approach to coverage and rate in cellular networks," *IEEE Transactions on Communications*, vol. 59, no. 11, pp. 3122–3134, 2011.

[27] J. G. Andrews, A. K. Gupta, and H. S. Dhillon, "A primer on cellular network analysis using stochastic geometry," 2016. [Online]. Available: https://arxiv.org/abs/1604.03183

Maurilio Matracia [S'21] received his M.Sc. degree in Electrical Engineering from the University of Palermo (UNIPA), Italy, in 2019. He is currently a Doctoral Student at the Communication Theory Lab (CTL), King Abdullah University of Science and Technology (KAUST), Kingdom of Saudi Arabia (KSA). His experience with IEEE includes serving as a reviewer for several journals and receiving prizes at the *SusTech 2021 student poster* as well as *ComSoc EMEA Region – Internet for All* contests. His main research interest is SG, with a special focus on rural and emergency communications.

Mustafa A. Kishk [S'16, M'18] Mustafa A. Kishk received the B.Sc. and M.Sc. degrees from Cairo University, Giza, Egypt, in 2013 and 2015, respectively, and the Ph.D. degree from Virginia Tech, Blacksburg, VA, USA, in 2018, all in Electrical Engineering. He is an assistant professor at the Electronic Engineering Department, Maynooth University, Ireland. Before that, he was a Postdoctoral Research Fellow with the Communication Theory Laboratory, King Abdullah University of Science and Technology, Saudi Arabia. He currently serves as an associate editor with IEEE Wireless Communication Letters. His current research interests include stochastic geometry, UAV-enabled communication systems, and satellite-enabled communications. He is a recipient of the IEEE ComSoc Outstanding Young Researcher Award for Europe, Middle East, and Africa Region, in 2022. He was recognized as an Exemplary Reviewer by the IEEE Communications Letters in 2020 and 2021.

Mohamed-Slim Alouini [S'94, M'98, SM'03, F'09] was born in Tunis, Tunisia. He received his Ph.D. degree in Electrical Engineering from California Institute of Technology (Caltech), Pasadena, CA, USA, in 1998. He served as a faculty member at the University of Minnesota, Minneapolis, MN, USA, then at Texas A&M University at Qatar, Education City, Doha, Qatar, before joining KAUST as a Professor of Electrical Engineering in 2009. His current research interests include the modeling, design, and performance analysis of wireless communication systems.